

# Oxidation Study of a Polycrystalline Ni/Cr Alloy II

Gar B. Hoflund\* and William S. Epling

Department of Chemical Engineering, University of Florida, Gainesville, Florida 32611

Received March 27, 1997. Revised Manuscript Received October 20, 1997<sup>⊗</sup>

The oxygen uptake of a sputtered and annealed polycrystalline Ni/Cr alloy surface has been examined using Auger electron spectroscopy (AES). The O<sub>2</sub> exposures were carried out at 10<sup>-7</sup> Torr and room temperature. Then the compositional and chemical-state changes induced at a 100-langmuir O<sub>2</sub>-exposed surface with increasing annealing times and temperatures were examined using AES, ion-scattering spectroscopy (ISS), and X-ray photoelectron spectroscopy (XPS). These three techniques probe different depths beneath the surface, so they provide depth-sensitive information about the complex chemical processes and compositional changes that occur during annealing. With annealing to 500 °C the near-surface region becomes enriched in Cr according to the ISS and AES data. XPS data indicate that Ni is present as Ni metal, NiO, and Ni(OH)<sub>2</sub> and that Ni metal is the predominant chemical state of Ni in the region probed by this technique. Cr is present as metallic Cr, CrO<sub>2</sub>, CrO<sub>3</sub>, Cr<sub>2</sub>O<sub>3</sub>, and Cr(OH)<sub>x</sub> with CrO<sub>2</sub> being the predominant chemical state below 500 °C. Both XPS and AES data indicate that NiO is reduced to Ni metal as Cr metal is oxidized to CrO<sub>x</sub>. Oxygen dissolution into the bulk of the sample occurs after annealing the sample at 500 °C or above. After a 650 °C anneal for 2 h, very little of the oxides remain in the near-surface region, but NiO and CrO<sub>x</sub> are still present in the subsurface region probed by XPS. The annealing treatments result in reversion of the O<sub>2</sub>-exposed surface nearly to the initially cleaned Ni/Cr surface.

## Introduction

Nichrome (Ni/Cr) alloys are technologically important in several applications. They are used as resistor elements in the electronics industries because they have a relatively large resistivity and a low-temperature coefficient of resistance.<sup>1–5</sup> Nichrome filaments also are used in certain high-temperature oxidizing environments because these alloys are more resistant to oxidation<sup>6</sup> than pure Ni. These properties are dependent upon the formative conditions, including the deposition environment and subsequent annealing treatments. For example, the stability of oxide films formed generally increases if an oxygen exposure–annealing cycle is used.

Jeng et al.<sup>7</sup> have carried out a study of polycrystalline and single-crystal Ni/Cr alloy surfaces to observe the changes induced by oxygen exposure and annealing using Auger electron spectroscopy (AES) and ion-scattering spectroscopy (ISS). They conclude that annealing at 500 °C results in migration of Cr to the near-surface region where it reacts with NiO to form Cr oxide. Annealing this surface for 4 h at 500 °C results in migration of oxygen from the near-surface region to the

subsurface region. Jeng et al.<sup>8</sup> also have carried out an X-ray photoelectron spectroscopy (XPS) study of the passivation of a Ni/Cr alloy surface at room temperature. They claim that Cr is oxidized preferentially to Cr<sub>2</sub>O<sub>3</sub> initially but that Ni in the alloy is oxidized more rapidly to NiO than Ni metal. Furthermore, they propose the presence of a layered structure consisting of a mixture of Ni hydroxide and Cr oxide, in the outermost atomic layer, a mixture of Cr oxide and small amounts of NiO and metallic Ni in the next four atomic layers, and a Cr-depleted layer beneath these two layers.

In this study the oxygen uptake during room-temperature, 10<sup>-7</sup>-Torr O<sub>2</sub> exposures has been examined using AES, and the changes that occur at the 100-langmuir O<sub>2</sub>-exposed Ni/Cr surface have been examined after various annealing treatments using AES, XPS, and ISS. These three surface characterization techniques probe different depths beneath the surface and, therefore, provide depth-sensitive compositional and chemical-state information as the sample is altered by annealing.

## Experimental Section

The polycrystalline Ni/Cr (23 at. % Cr) sample used in this study was prepared from 99.99% pure Ni and Cr purchased from A. D. McKay. This alloy composition was chosen so that comparisons could be made with the results of previous Ni/Cr studies.<sup>7–10</sup> The pure elements were melted in a cold-hearth,

<sup>⊗</sup> Abstract published in *Advance ACS Abstracts*, December 15, 1997.  
(1) Au, C. L.; Jackson, M. A.; Anderson, W. A. *J. Electron. Mater.* **1987**, *16*, 301.

(2) Nocerino, G.; Singer, K. E. *J. Vac. Sci. Technol.* **1979**, *16*, 147.

(3) Hofmann, S.; Zalar, A. *Thin Solid Films* **1976**, *39*, 219.

(4) Lassak, L.; Hieber, K. *Thin Solid Films* **1973**, *17*, 105.

(5) Koltai, M.; Trifonov, I.; Czermann, M. *Vacuum* **1983**, *33*, 49.

(6) Kubaschewski, O.; Hopkins, B. E. *Oxidation of Metals and Alloys*; Butterworth: London, 1962.

(7) Jeng, S. P.; Holloway, P. H.; D. A. Asbury, D. A.; Hoflund, G. B. *Surf. Sci.* **1990**, *235*, 175.

(8) Jeng, S. P.; Holloway, P. H.; Batich, C. D. *Surf. Sci.* **1990**, *227*, 278.

(9) Steffen, J.; Hofmann, S. *Surf. Interface Anal.* **1988**, *11*, 617.

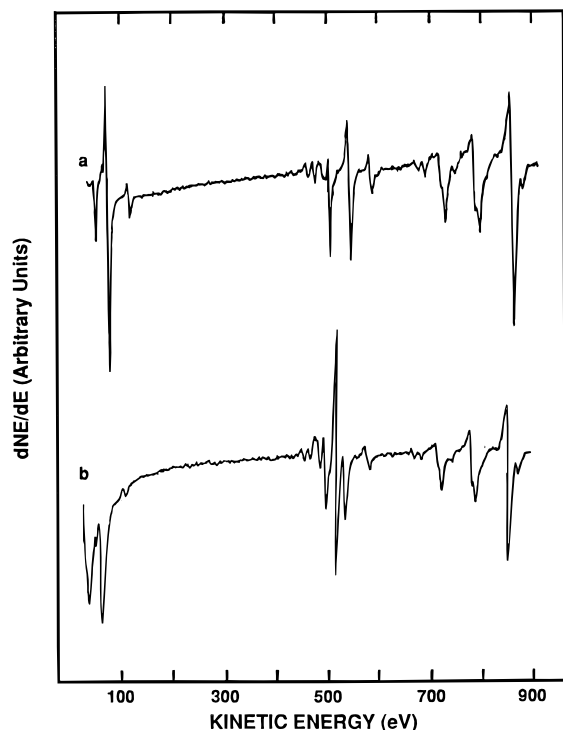


**Figure 1.** Auger spectra obtained from (a) the cleaned Ni/Cr surface and (b) the room temperature 100-langmuir oxygen-exposed polycrystalline Ni/Cr sample.

mono-arc melter which had been evacuated to approximately  $10^{-5}$  Torr and backfilled with high-purity Ar. Slices of the polycrystalline alloy boules of about 1 cm in diameter and 1 mm in thickness were cut and polished using standard metallographic techniques.

The sample was then introduced into an ultrahigh-vacuum system (base pressure  $10^{-11}$  Torr). After pumpdown it was sputtered and annealed until no contaminants were observable by AES. Immediately before the oxidation experiments, the sample was sputter cleaned, annealed at 650 °C for 30 min, and then cooled to room temperature. Dosing with O<sub>2</sub> was performed at a pressure of  $10^{-7}$  Torr.

AES, ISS, and XPS were performed using a double-pass cylindrical mirror analyzer (CMA) (Perkin-Elmer PHI model 15-255GAR). AES data were collected by operating the CMA in a nonretarding mode, using analogue detection and a primary electron beam energy of 3 keV. The beam current was 10  $\mu$ A over a 0.5 mm diameter spot size. ISS was performed using a 1-keV Ne<sup>+</sup> beam at a current of 100 nA over a spot size of about 5 mm. A 148° scattering angle was used, the CMA was operated in the nonretarding mode using pulse counting detection,<sup>11</sup> and each spectrum was collected in 90 s. These parameters result in negligible surface damage. XPS data were collected using Mg K $\alpha$  X-rays as the excitation source. The CMA was operated in the retarding mode with a pass energy of 25 eV, and pulse counting detection was used. In this study the sample normal was oriented at an angle of 30° with respect to the CMA axis.

## Results and Discussion

Auger spectra taken from the cleaned Ni/Cr alloy surface before and after a 100-langmuir exposure to O<sub>2</sub> at room temperature are shown in Figure 1a,b, respectively, and the oxygen uptake according to AES is shown in Figure 2. The features in Figure 1a are characteristic

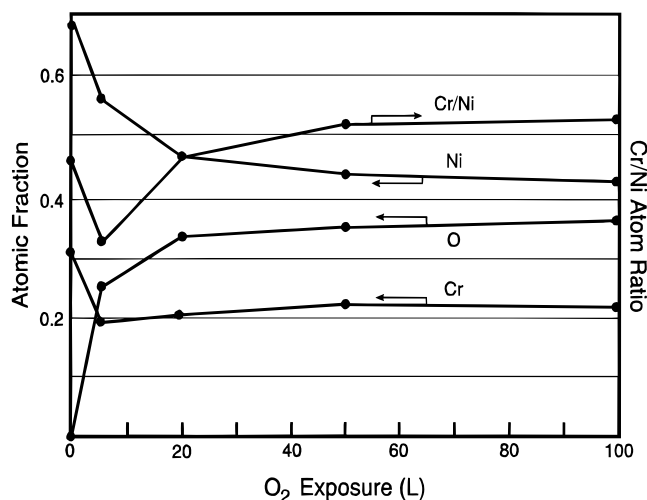


**Figure 2.** Near-surface concentrations of the Ni/Cr alloy and the Ni/Cr atomic ratio as a function of O<sub>2</sub> exposure at room temperature. The concentrations were calculated using an Auger peak-height analysis of the O and Cr features just above 500 eV<sup>12</sup> based on the assumption that the composition in the near-surface region is homogeneous.

of those obtained from pure metallic Cr and Ni.<sup>12</sup> Upon oxidation or with annealing, the Cr 571 eV feature does not exhibit a significant peak-shape change. This implies that the peak height of this feature can be used for quantification of the Auger data using published sensitivity factors and the assumption that the composition of the near-surface region is homogeneous.<sup>12</sup> On the basis of the results of the previous studies,<sup>7,8</sup> this assumption is known to be incorrect in this case. Nevertheless, the calculated depth profiles obtained from Auger data based on this assumption are useful for qualitatively assessing migration of species within the near-surface region. The calculated composition of the cleaned Ni/Cr surface is 68 at. % Ni and 32 at. % Cr, which indicates that the near-surface region is enriched in Cr compared to the bulk value of 23 at. %. With increasing exposure the O concentration initially increases rapidly and then slowly above an exposure of 20 langmuirs. This curve is very similar to the uptake curve based on XPS data presented by Jeng et al. (Figure 1 of ref 8) and AES data obtained by Steffen and Hofmann.<sup>9</sup> The Ni concentration decreases monotonically over the 0–100 langmuir O<sub>2</sub> exposure range, but the Cr concentration initially decreases during the 5-langmuir exposure and then slowly increases with increasing exposure. The fact that the Cr concentration increases only slightly rather than decreases as large amounts of oxygen are incorporated into the sample over the exposure range of 5–100 langmuir of O<sub>2</sub> indicates that there is preferential migration of the Cr toward the surface with increasing oxidation at room temperature. The 100-langmuir O<sub>2</sub> exposure results in the presence of a large O KLL Auger feature at 512 eV and a calculated near-surface composition of 42 at. % Ni, 22 at. % Cr, and 36 at. % O. Angle-resolved AES studies by Hoflund and co-workers<sup>13,14</sup> demonstrate that AES

(10) Mathieu, H. J.; Landolt, D. *Corros. Sci.* **1986**, *26*, 547.

(11) Gilbert, R. E.; Cox, D. F.; Hoflund, G. B. *Rev. Sci. Instrum.* **1981**, *18*, 56.

(12) Davis, L. E.; MacDonald, N. C.; Palmberg, P. W.; Riach, G. E.; Weber, R. E. *Handbook of Auger Electron Spectroscopy*, Physical Electronics Industries, Eden Prairie, MN, 1976.

(13) Hoflund, G. B.; Asbury, D. A.; Corallo, C. F.; Corallo, G. R. *J. Vac. Sci. Technol. A* **1988**, *6*, 70.

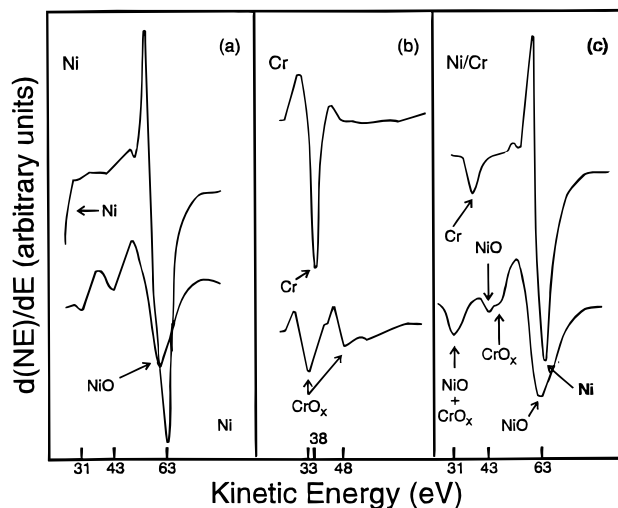


**Figure 3.** Low-energy Auger spectra obtained from (a) polycrystalline Ni, (b) polycrystalline Cr, and (c) a Ni/Cr alloy (110) surface before and after a 200-langmuir  $O_2$  exposure at room temperature. This figure has been reproduced from ref 7 with permission.

probes quite deeply beneath the surface ( $\sim 30$  atomic layers or  $40 \text{ \AA}$ ) when the kinetic energies of the Auger electrons are  $400 \text{ eV}$  or greater. Less than 10% of the Auger signal originates from the outermost atomic layer.

The low kinetic energy features, however, involve valence-level electrons so their positions and peak shapes are highly sensitive to Ni- and Cr-chemical state changes. Jeng et al.<sup>7</sup> have shown detailed peak shapes of features with kinetic energies below  $80 \text{ eV}$  from metallic Ni, metallic Cr, and Ni/Cr(110) before and after exposure to 200 langmuir of  $O_2$  at room temperature and have presented an explanation of the origin of the observed features. This information is important with regard to understanding the Auger spectra presented in this study, and thus Figure 1 from the study by Jeng et al.<sup>7</sup> is reproduced in Figure 3. Metallic Ni exhibits a large feature at a kinetic energy of  $63 \text{ eV}$  and a smaller feature at about  $23 \text{ eV}$ . Only an edge of this latter feature is observable in Figure 3, but the feature has been published previously.<sup>12</sup> Oxidation diminishes the intensities of these peaks significantly, particularly the portions above the baseline for the  $63 \text{ eV}$  peak which is also broadened and shifted slightly to lower energy. Two smaller features become apparent at  $31$  and  $43 \text{ eV}$ . The low kinetic-energy region of the metallic Cr region consists of a well-defined peak at  $38 \text{ eV}$ , and oxidation results in loss of this peak and formation of two smaller features at  $33$  and  $48 \text{ eV}$ . Oxidation of the Ni/Cr(110) surface results in peaks due to both Cr oxides and Ni oxide, but several of the features are difficult to resolve due to the close proximity of the peaks. Fortunately, the instrumental resolution is high in this kinetic energy range because these data are collected in the nonretarding mode. In this mode the CMA band-pass is small because it is directly proportional to the electron kinetic energy which is small for these Auger features. In addition to their high resolution and sensitivity to chemical state, these Auger features are very surface specific because their kinetic energies lie near to mini-

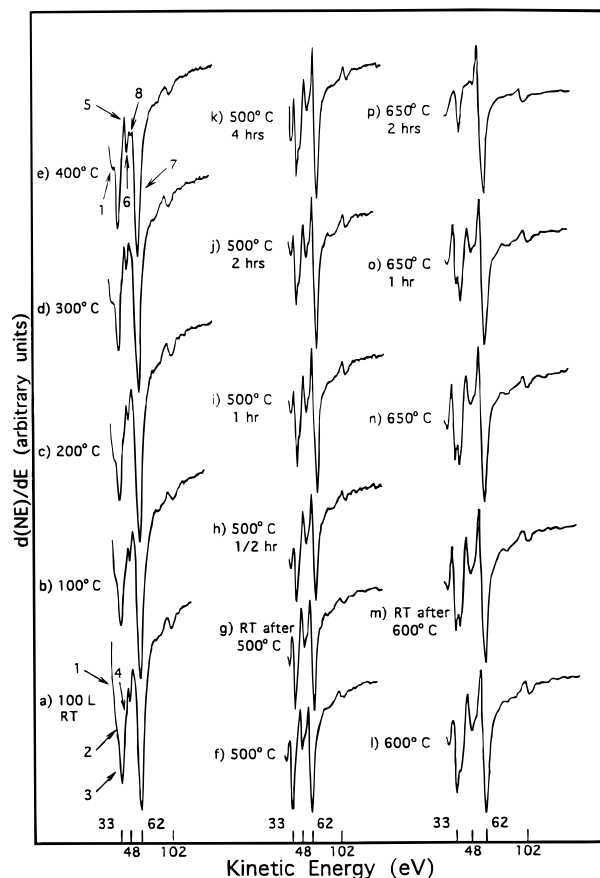


**Figure 4.** Low kinetic energy Auger spectra taken after the annealing treatments shown by the spectra.

**Table 1. Low-Energy Auger Peak Assignments**

kinetic energy (eV)	Figure 3 arrow no.	species
24	1	Ni metal
31	2	NiO
33	3	$CrO_x$
38	4	Cr metal
43	5	NiO
48	6	$CrO_x$
62, 63	7	NiO, Ni metal
53	8	$CrO_x$

um of the universal mean-free-path (mfp) curve<sup>15</sup> with a mfp of about  $0.4 \text{ nm}$ . Thus, most of this signal originates within the eight outermost atomic layers.

Low-energy Auger spectra obtained from the 100-langmuir  $O_2$ -exposed Ni/Cr surface before and after annealing at different temperatures for varying times are shown in Figure 4. Eight peaks (or shoulders) with kinetic energies below  $70 \text{ eV}$  are present in all of these spectra. These features are marked with numbered arrows in Figure 4a,e, and the assignments, based on the discussion above, are given in Table 1. The subtle features in Figure 4 discussed below are apparent when full-scale spectra are overlaid.

The low-energy portion of the Auger spectrum taken from the 100-langmuir  $O_2$ -exposed sample is shown in Figure 4a. The  $62 \text{ eV}$  Ni peak resembles an oxidized Ni feature (arrow 7), and the small  $48 \text{ eV}$  peak located between the two large peaks and assigned to  $CrO_x$  (arrow 6) is also evident. The  $24\text{-eV}$  Ni metal peak (arrow 1) and the  $31\text{-eV}$  NiO peak (arrow 2) are barely

(14) Davidson, M. R.; Hoflund, G. B.; Outlaw, R. A. *J. Vac. Sci. Technol. A* **1991**, *9*, 1344.

(15) Palmberg, P. W. *Anal. Chem.* **1973**, *45*, 549A.

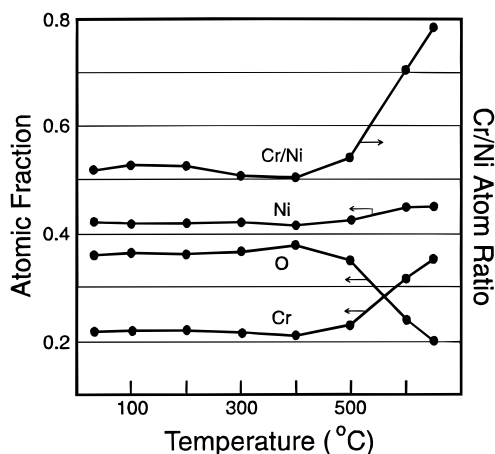


**Figure 5.** Near-surface concentration of the Ni/Cr alloy as a function of annealing temperature. The concentrations were calculated using an Auger peak-height analysis<sup>12</sup> based on the assumptions that the concentration in the near-surface region is homogeneous and the peak shape changes are negligible. The Cr/Ni atomic concentration ratio is also shown.

distinguishable as shoulders due to overlap with the Cr features. The large low kinetic energy feature has an energy that lies between the 38 eV metal peak and the 33 eV oxide peak (arrow 3), indicating that a mixture of Cr states is present. Although most of the Cr is oxidized, a shoulder due to metallic Cr (arrow 4) is apparent. A 43-eV feature due to NiO (arrow 5) cannot be discerned in these spectra. An Auger spectrum taken after annealing the 100-langmuir exposed surface at 100 °C is shown in Figure 4b. The large  $\text{CrO}_x$  feature is shifted to 33 eV, indicating that metallic Cr in the near-surface region becomes more fully oxidized during the 100 °C anneal. A subtle shoulder is still present at 38 eV, indicating that some Cr remains in metallic form. The Ni features are not changed. The spectrum shown in Figure 4c was obtained after heating the sample to 200 °C. The shoulder at 38 eV associated with Cr metal is decreased slightly in intensity implying that either the Cr metal migrates into the subsurface region or that more of the Cr is oxidized during the 200 °C anneal. Jeng et al.<sup>7</sup> suggest that Cr migrates from the bulk into the near-surface region and is oxidized as NiO is reduced at 500 °C. The peak at 48 eV appears to be slightly enhanced due to formation of  $\text{CrO}_x$ , and this trend continues in Figure 4d,e. In Figure 4e the small indentation between the 48 and 62 eV peaks (arrow 8 in Figure 4e) is associated with the 48-eV  $\text{CrO}_x$  peak as observed in Figure 3. Further support of the assertion that  $\text{CrO}_x$  forms as NiO is reduced is provided by the fact that the Cr metal feature at 38 eV becomes less prominent with annealing in Figure 4a–e. With annealing the large structure at 33 eV generally becomes narrower and more well defined. This trend suggests that several chemical states of Cr are present initially and that annealing results in conversion to some particular oxide chemical state. The XPS data discussed below confirm this assertion. The compositions of the near-surface region calculated from the higher energy Auger peaks are shown in Figure 5 as a function of annealing temperature. There is essentially no compositional change with annealing to 400 °C.

The Auger spectrum collected while annealing the sample at 500 °C is shown in Figure 4f. The  $\text{CrO}_x$  peak

at 48 eV and its associated peak at a slightly higher kinetic energy are increased significantly in intensity. The 33 eV Cr oxide feature is now quite well defined as is the 24-eV Ni metal peak, and the shape of the 62-eV peak is more metallic like. These changes indicate that the reaction between Cr and NiO to form Ni and  $\text{CrO}_x$  is more complete. After the sample was allowed to cool to room temperature, the spectrum in Figure 4g was taken. The Cr oxide concentration in the near-surface region is decreased relative to the Cr metal concentration, and the Cr peak at 33 eV is increased in size relative to the 62-eV Ni peak. This is due to migration of Cr to the near-surface region as oxygen simultaneously migrates away from the surface. Reheating the sample to 500 °C and allowing it to remain at that temperature for 0.5, 1, 2, and 4 h results in the spectra shown in Figure 4h–k, respectively. Although the oxides are still the predominant states, more metallic Cr and Ni accumulate in the near-surface region with annealing time. No desorption of O was observed during this period using a quadrupole mass spectrometer. This supports the assertion that oxygen migrates toward the bulk during these treatments. Further support is gained from the concentration profiles shown in Figure 5 as discussed below. Ni metal probably forms during this annealing treatment by reaction of Cr metal with NiO. Jeng et al.<sup>7</sup> conclude that Cr oxide migrates into the subsurface region of a Ni/Cr(110) sample after a 4-h 500 °C anneal, which agrees with the data obtained in this study.

The spectra taken from the Ni/Cr sample after it was heated to 600 °C and allowed to cool to room temperature are shown in Figures 4l,m, respectively. The high-temperature anneal apparently does not affect the peak shapes compared to the 500 °C spectra. Upon cooling to room temperature, the metallic Cr feature is significantly increased due to migration of Cr to the near-surface region and oxygen away from the surface. More metallic Ni is also present as evidenced by the increased sizes of the 24 and 62 eV peaks. The spectra taken after heating the sample to 650 °C and then annealing at that temperature for 1 and 2 h are shown in Figure 4n–p, respectively. In all of these spectra, the Cr metal peak is more intense than the  $\text{CrO}_x$  peak due to further migration of oxygen into the subsurface region and Cr toward the surface. Annealing the sample for 2 h at 650 °C results in essentially complete migration of oxygen beneath the surface region probed by AES according to the spectrum shown in Figure 4p. The low-energy features now resemble the features obtained from a clean Ni/Cr sample. The complete Auger spectrum taken from this sample is shown in Figure 6. It is nearly identical with the spectrum obtained from the cleaned Ni/Cr alloy surface shown in Figure 1a. The oxygen Auger peak at 512 eV is slightly larger in Figure 6. In both cases this oxygen is subsurface as discussed below in conjunction with the ISS and XPS data. The changes exhibited in Figure 4e–p correlate with the compositional trends shown in Figure 5 over the temperature range 400–650 °C. The near-surface region is enriched in both Cr and Ni metal but much more so for the Cr metal. The oxygen content decreases almost by a factor of 2. The Cr/Ni ratio at 650 °C is equal to

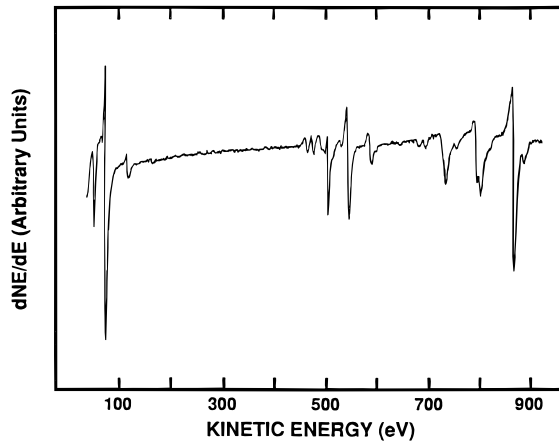


**Figure 6.** Auger spectrum obtained from the 100-langmuir  $O_2$ -exposed Ni/Cr surface after annealing at 650 °C for 2 h.

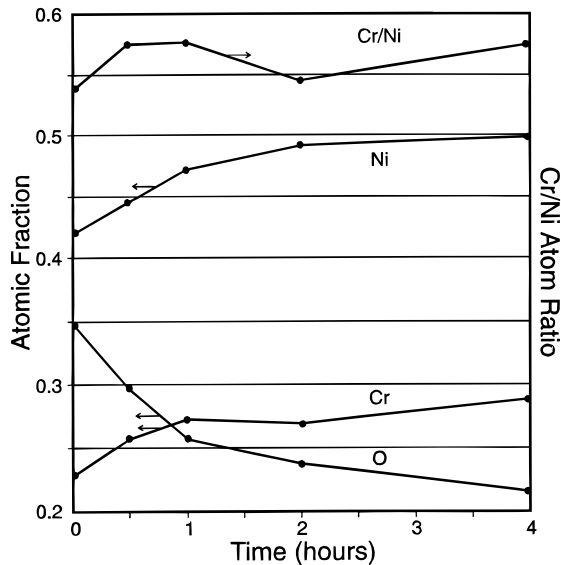


**Figure 7.** Near-surface composition of the  $O_2$ -dosed Ni/Cr alloy determined from AES data as a function of annealing time at 500 °C. The Cr/Ni atomic concentration ratio is also shown.

0.78, which is considerably larger than the value of 0.47 for the initially cleaned surface (Figure 1a).

The compositions and Cr/Ni atom ratios are shown as a function of annealing time at 500 and 650 °C in Figures 7 and 8, respectively. The data shown in Figure 7 indicate that the Cr and Ni concentrations both increase with annealing time while the O concentration decreases. The Cr concentration increases from 23 to 28 at. % and the Ni concentration increases from 42 to 50 at. %, which are both significant increases. During this treatment, the Cr/Ni ratio remains relatively constant. According to the data shown in Figure 8, annealing at 650 °C for 2 h results in nearly complete migration of the oxygen into the subsurface region according to AES. The Cr concentration decreases only slightly from 43 to 41 at. % while the Ni concentration increases significantly from 44 to 68 at. %. This results in a decrease of the Cr/Ni ratio from 0.78 to 0.57 compared to 0.52 for the oxygen-exposed Ni/Cr surface. Thus, the initial surface becomes Cr rich by annealing to 650 °C and then returns almost to its original clean composition by annealing at 650 °C for 2 h. These

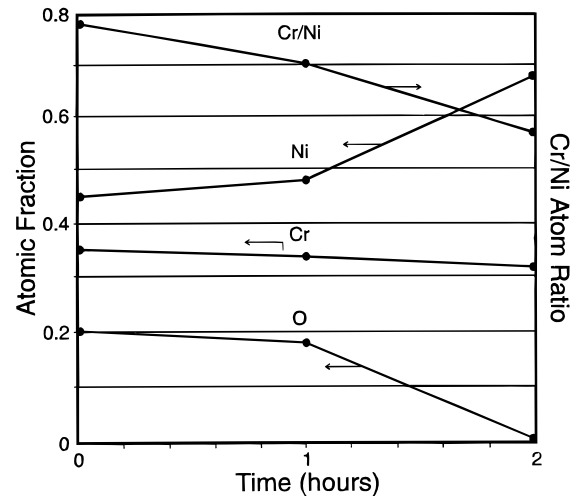


**Figure 8.** Near-surface composition of the  $O_2$ -dosed Ni/Cr alloy determined from AES data as a function of annealing time at 650 °C. The Cr/Ni atomic concentration ratio is also shown.

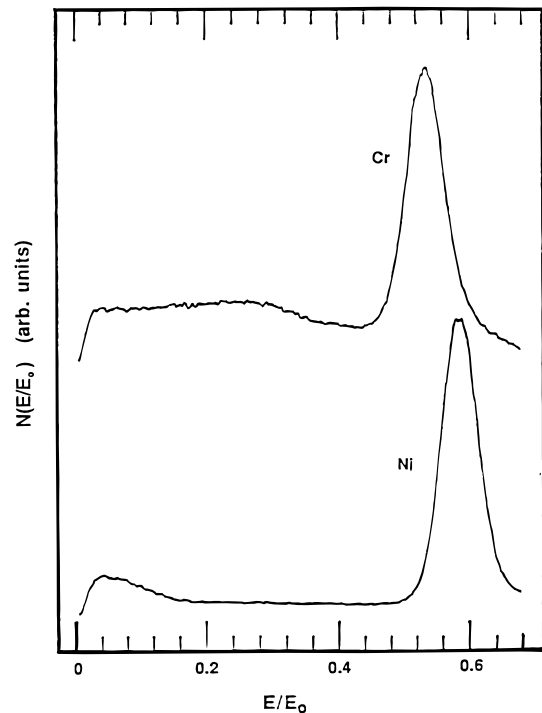


**Figure 9.** ISS spectra taken from sputter-cleaned polycrystalline Cr and Ni surfaces.

compositional trends also are consistent with the low kinetic energy Auger data presented in Figure 4.

ISS spectra taken from polycrystalline Ni and Cr and the Ni/Cr alloy are shown in Figures 9 and 10, respectively. ISS data provide compositional information about the outermost atomic layer. It is so highly surface sensitive because ions that penetrate beneath the surface are either neutralized or scattered multiple times in which case they do not contribute to elemental peaks. ISS spectra obtained from the cleaned Ni/Cr alloy surface before and after exposure to 100 langmuirs of  $O_2$  at room temperature are shown in Figure 10a,b respectively, and ISS data obtained after annealing the sample to 500 °C for 0, 1/2, 1, 2 and 4 h are shown in Figure 10c–g, respectively. Young and Hoflund<sup>16</sup> have developed a numerical method for curve-resolving ISS

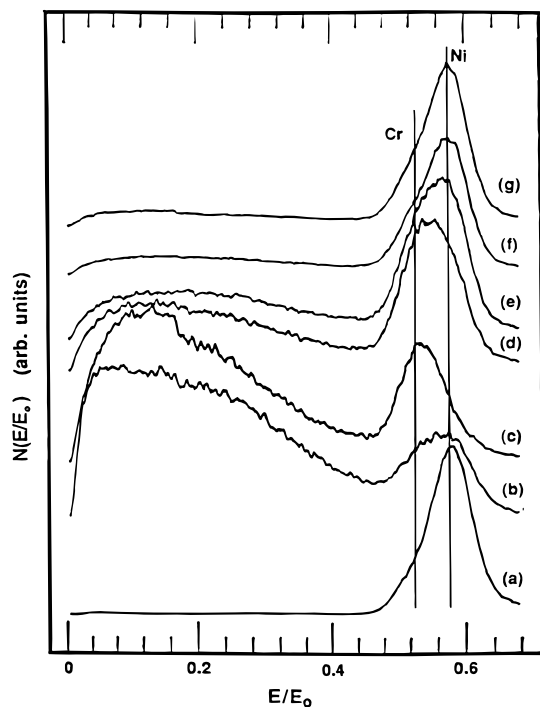


**Figure 10.** ISS spectra taken from the Ni/Cr alloy surface using 1-keV  $\text{Ne}^+$  (a) after cleaning, (b) after dosing with 100 langmuirs of  $\text{O}_2$  at room temperature, (c) immediately after heating the dosed sample to 500 °C, and after annealing the dosed sample at 500 °C for (d)  $1/2$ , (e) 1, (f) 2, and (g) 4 h. This figure has been reproduced from ref 7 with permission.

features when the elements have similar masses. This method takes the isotopic distributions of the elements into account and utilizes a linear background subtraction. This method and the elemental peak shapes shown in Figure 9 were used to obtain the curve-resolved features shown in Figure 11. The outermost atomic layer compositions were calculated assuming that the ISS sensitivity factors are similar for Ni and Cr. This is reasonable because their masses are similar. The results of this analysis are given in Table 2. The oxygen fraction of the outermost atomic layer was calculated by dividing the Cr plus Ni signal from a given surface by the Cr plus Ni signal obtained from the clean surface and subtracting this value from 1.0. This assumes that the neutralization probability does not depend upon surface oxygen content. This may not be accurate because the ion neutralization efficiency depends upon the electrical properties of the surface and specifically the conductivity. The surface conductivity depends upon the free electron density and electron mobility, which may vary with oxygen content. In this ISS experiment a well-defined peak is not obtained for oxygen because the  $\text{Ne}^+$  is more massive than O. However, a large, poorly defined background is apparent in Figure 10 over an  $E/E_0$  from 0 to 0.48 for the oxygen-containing surfaces. The size of this feature decreases as the outermost atomic oxygen content decreases so it is attributed to oxygen.

The cleaned surface contains 22 at. % Cr with a Cr/Ni ratio of 0.28, which is similar to the bulk composition. After the 100-langmuir  $\text{O}_2$  exposure, 82% of the outermost atomic layer is oxygen and the Cr/Ni ratio is 1.0.

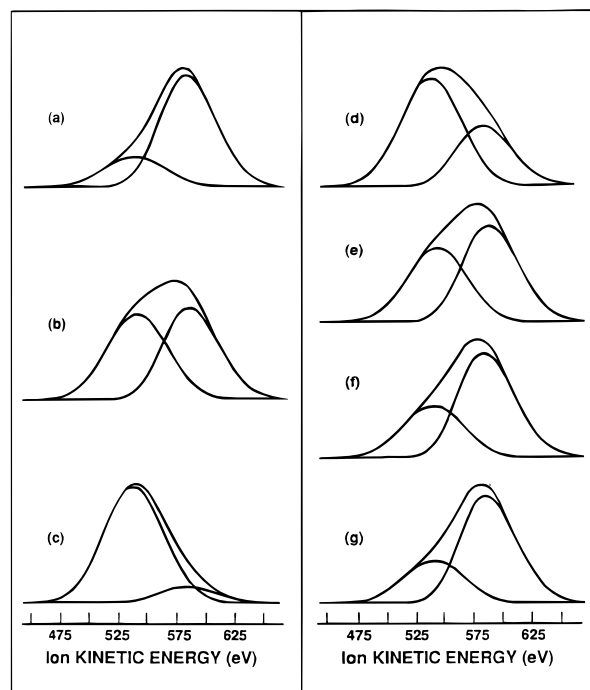


**Figure 11.** Resolved Ni and Cr ISS features after background subtraction corresponding to the experimental data shown in Figure 10.

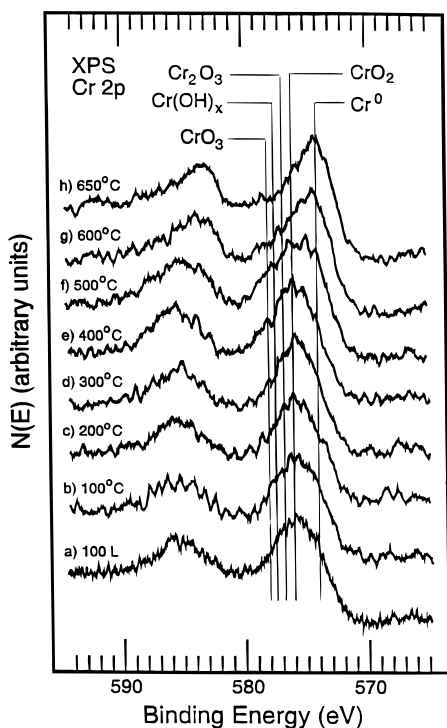
This is considerably higher than the value of 0.52 determined by AES which probes much more deeply than ISS. Immediately after heating to 500 °C, the oxygen content does not change significantly, but the Cr/Ni ratio is increased to 7.0. This indicates that Cr migrates to the outermost surface layer during heating to 500 °C. The corresponding Cr/Ni ratio determined by AES is increased only to 0.54. An explanation consistent with these facts is that only Cr located very near to the surface migrates to the outermost surface layer.

An interesting trend occurs with annealing time at 500 °C. The O content decreases very significantly from 84 to 25 at. %, the Cr content remains fairly constant at about 20 at. %, and the Ni content increases quite significantly from 2 to 52 at. %. These latter two facts result in a monotonic decrease in the Cr/Ni ratio from 7.0 to 0.4 as observed in Table 2 and Figure 11c–g. It is clear by the trends in Table 2 and Figures 10 and 11 that the outermost atomic layer of the surface is reverting to its initial state with annealing time at 500 °C according to the ISS data. This same process is apparent in the Auger data but at 650 °C as discussed above.

An XPS Cr 2p spectrum taken from the 100-langmuir  $\text{O}_2$ -dosed Ni/Cr sample is shown in Figure 12a. The XPS binding energies are given in Table 3. A mixture of Cr states is present which may include metallic Cr,  $\text{CrO}_2$ ,  $\text{Cr}_2\text{O}_3$ ,  $\text{Cr}(\text{OH})_x$ , and  $\text{CrO}_3$  with  $\text{CrO}_2$  as the predominant state. The Cr 2p peaks are rather broad and not well-defined, so it is difficult to make specific statements regarding which oxides contribute to the signal. Nevertheless, trends can be observed. The spectra shown in Figure 12b–h were taken after heating the sample to 100, 200, 300, 400, 500, 600, and 650 °C, respectively. The amount of  $\text{Cr}(\text{OH})_x$  present is somewhat decreased after heating to 100 °C and is decreased

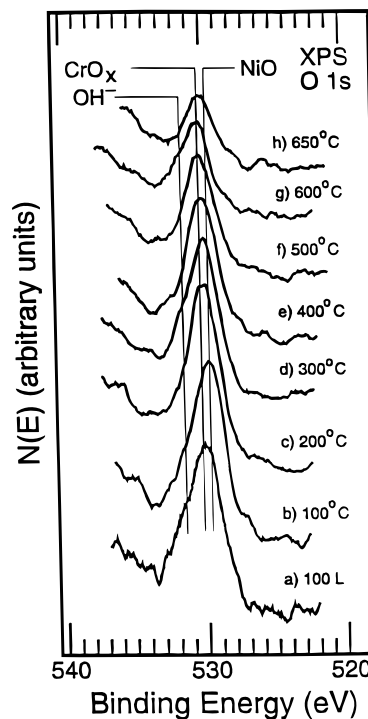
**Table 2. Ni/Cr Alloy ISS Surface Compositions (at. %)**

	Figure 10						
	a	b	c	d	e	f	g
annealing temp (°C)	cleaned surface	32 (100-langmuir O <sub>2</sub> dose)	500	500	500	500	500
annealing time (h)	0	0	0	0.5	2.0	2.0	4.0
composition:							
0	0	82	84	70	61	36	25
Cr	22	9	14	20	18	22	23
Ni	78	9	2	10	21	42	52
Cr/Ni ratio	0.28	1.0	7.0	2.0	0.86	0.52	0.44

**Figure 12.** Cr 2p XPS spectra obtained (a) from the oxidized sample and after heating to (b) 100, (c) 200, (d) 300, (e) 400, (f) 500, (g) 600, and (h) 650 °C.**Table 3. XPS Binding Energies**

chemical state	binding energy
Cr 2p <sub>3/2</sub>	
Cr metal	574.0
CrO <sub>2</sub>	576.0
Cr <sub>2</sub> O <sub>3</sub>	576.8
CrO <sub>3</sub>	578.0
Cr(OH) <sub>x</sub>	577.4
Ni 2p <sub>3/2</sub>	
Ni metal	852.5
NiO	854.0
Ni(OH) <sub>2</sub>	855.5
O 1s	
Cr <sub>2</sub> O <sub>3</sub>	530.2
CrO <sub>3</sub>	530.2
NiO	529.7
OH <sup>-</sup>	531.2

further with each heating step at higher temperatures. The decrease is due to desorption of H-containing species at higher temperatures. Hydrogen is present in the background of UHV systems and readily adsorbs on Ni which possibly accounts for its presence. The metallic Cr content remains unchanged at 100 °C, but it decreases as the sample is heated to 200, 300, and 400 °C. Throughout this temperature range a well-defined Cr<sub>2</sub>O<sub>3</sub> shoulder is present, and CrO<sub>2</sub> remains the predominant state of Cr. Significant chemical

**Figure 13.** O 1s XPS spectra obtained (a) from the oxidized sample and after heating to (b) 100, (c) 200, (d) 300, (e) 400, (f) 500, (g) 600, and (h) 650 °C.

changes occur while heating the sample from 400 to 500 °C. A well-defined CrO<sub>3</sub> shoulder becomes apparent, the Cr metal concentration is increased, and the Cr<sub>2</sub>O<sub>3</sub> and CrO<sub>2</sub> contributions are decreased. These changes are consistent with the suggestion that a disproportionation reaction occurs in which Cr<sub>2</sub>O<sub>3</sub> and/or CrO<sub>2</sub> decomposes to Cr metal and CrO<sub>3</sub>. At 600 °C the CrO<sub>3</sub> feature is smaller, but the asymmetry on the higher binding energy side is still present, and the Cr<sub>2</sub>O<sub>3</sub> peak is also reduced in size. The binding energy of the predominant peak is shifted to a lower binding energy as metallic Cr becomes the predominant chemical state. This trend is continued at 650 °C. Cr metal is the predominant chemical state, but a small amount of CrO<sub>2</sub> remains in the region probed by XPS and contributes a shoulder to the Cr 2p spectrum. This is in agreement with the AES data presented above where Cr and Ni metals were the only species present. However, since the region probed by XPS contains deeper layers than AES due to mean-free-path differences, the oxides observed in Figure 12h lie beneath the AES detection region.

The corresponding XPS O 1s peaks are shown in Figure 13. Features due to NiO, CrO<sub>x</sub>, and both Ni(OH)<sub>2</sub> and Cr(OH)<sub>x</sub> are apparent in these spectra. In Figure 13a the predominant feature is due to CrO<sub>x</sub>, but

large shoulders due to the presence of Cr and Ni hydroxides and NiO are also present. A more recent O 1s BE value of 531.6 eV has been published for Cr<sub>2</sub>O<sub>3</sub>.<sup>17</sup> If correct, this value is close to that of OH<sup>-</sup> and may also contribute to the intensity of this feature. After heating at 100 °C (Figure 13b), the NiO feature is predominant and the OH<sup>-</sup> shoulder is reduced in size. In both of these spectra, a mixture of Cr oxides and Ni oxide contributes to the O 1s feature in similar amounts. The changes that occur with annealing are reproducible, indicating that there are shifts between the predominant oxide form. As the temperature is increased to 600 °C, the peak maximum shifts toward higher binding energy, and the CrO<sub>x</sub> again becomes predominant. This is consistent with the assertion that NiO is reduced through formation of CrO<sub>x</sub> at elevated temperature. The shoulder due to OH<sup>-</sup> is quite prominent after heating at 300 °C, and then it is reduced in size. This could be due to migration of subsurface hydrogen to the surface at 300 °C and then desorption of water at 400 °C. The total area under the O 1s feature also decreases in magnitude after heating to 600 and 650 °C. This fact is consistent with the assertion that NiO decomposes as CrO<sub>x</sub> forms and that the CrO<sub>x</sub> decomposes forming O, which migrates toward the bulk. Another feature is present in these spectra at a binding energy of 528.0 eV. This is not due to the presence of Cr or Ni oxide or hydroxide. Initially, it is a large shoulder (Figure 13a) which decreases in prominence with heating to 500 °C and then increases again at 600 °C and even more so at 650 °C. This feature is believed to originate from chemisorbed oxygen. As the sample is heated to 500 °C, this oxygen is converted to an oxide, which explains the decreasing size of the shoulder. This is also consistent with the formation of more well-defined low-energy Auger features (Figure 4) as the sample is heated to 500 °C. At 600 and 650 °C the oxides decompose again, forming chemisorbed oxygen which migrates toward the bulk. This explains both the increase in the size of this shoulder at these temperatures and the decreasing XPS O 1s peak area. A feature with a similar binding energy has been observed in thermal decomposition studies of AgO and Ag<sub>2</sub>O.<sup>18,19</sup>

The corresponding XPS Ni 2p spectra are shown in Figure 14. The spectrum taken from the 100-langmuir, O<sub>2</sub>-dosed Ni/Cr surface is shown in Figure 14a. This spectrum is very similar to a spectrum presented by Jeng et al.<sup>8</sup> obtained from a polycrystalline Ni/Cr surface that had been given a similar treatment. Most of the Ni is present in the metallic state. Therefore, a considerably larger fraction of the Cr present in the near-surface region is oxidized compared to Ni. Annealing at higher temperatures results in reduction of both the Ni(OH)<sub>x</sub> and NiO features. The hydroxide feature is eliminated by heating to 400 °C, but a small amount of NiO remains even after heating to 650 °C according to XPS. The assignment of the Ni as well as the Cr species to oxide or hydroxide states and not mixed oxide species seems reasonable since the assignments match the spectral features and no unexplained features are

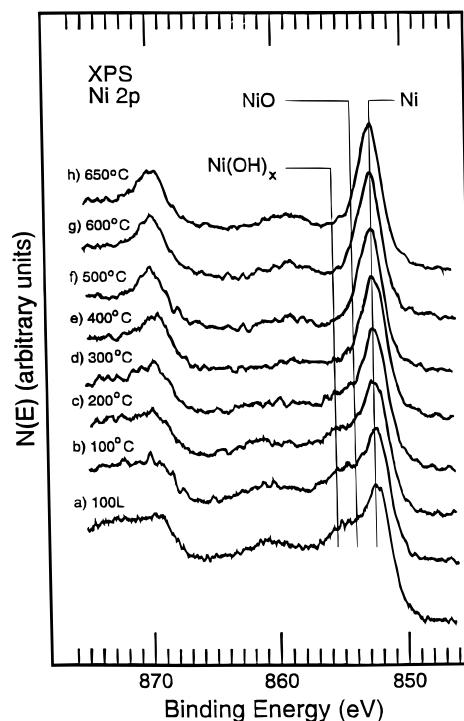


**Figure 14.** Ni 2p XPS spectra obtained (a) from the oxidized sample and after heating to (b) 100, (c) 200, (d) 300, (e) 400, (f) 500, (g) 600, and (h) 650 °C.

apparent. Although no evidence of mixed oxide species is apparent in the XPS data, small amounts of such species may be present.

XPS valence-band spectra were taken from the 100-langmuir, O<sub>2</sub>-exposed Ni/Cr surface before and after annealing at 650 °C (not shown). Before annealing the high-lying core-level O 2s peak is present at about 21 eV. There is also an increased density of states (DOS) in the range 4–14 eV beneath the Fermi level, which is probably due to mixing of the O 2p electrons with valence bonding levels of Cr and Ni. After annealing the spectral features due to oxygen are diminished. This fact is consistent with the other XPS and AES data, which indicate that oxygen migrates toward the bulk during annealing at high temperature.

## Summary

A polycrystalline Ni/Cr alloy was exposed to 100 langmuirs of O<sub>2</sub> at room temperature. It was then annealed at increasing temperatures for various time periods and examined using AES, XPS, and ISS to characterize the chemical and compositional changes that occur. The low kinetic energy Cr and Ni Auger features indicate that as the temperature rises to 500 °C, Cr migrates toward the surface and becomes oxidized as NiO is reduced. With annealing at 500 °C for 1 h and longer, the CrO<sub>x</sub> concentration in the near-surface region decreases as the CrO<sub>x</sub> decomposes and the oxygen migrates toward the bulk. The Cr/Ni ratio increases significantly with heating from 500 to 650 °C but decreases with time while annealing at 650 °C. The ISS data indicate that Cr migrates to the outermost atomic layer during the lower temperature treatments and then migrates toward the bulk as the surface

(17) Moulder, J. F.; Stickle, W. F.; Sobol, P. E.; Bomben, K. D. *Handbook of X-ray Photoelectron Spectroscopy*; Chastain, J., Ed.; Perkin-Elmer Corporation: Eden Prairie, MN, 1992.

(18) Weaver, J. F.; Hoflund, G. B. *J. Phys. Chem.* **1994**, *98*, 8519.

(19) Weaver, J. F.; Hoflund, G. B. *Chem. Mater.* **1994**, *6*, 1693.



oxygen content decreases with annealing at 500 °C. XPS data indicate that NiO is reduced as the temperature increases. The Cr is present as metallic Cr, CrO<sub>2</sub>, Cr<sub>2</sub>O<sub>3</sub>, CrO<sub>3</sub> and Cr(OH)<sub>x</sub>. Below 500 °C the Cr oxide decomposes to dissolved oxygen which migrates away from the surface. Annealing at 650 °C for 2 h produces a Ni/Cr surface which is quite similar to the initially cleaned surface.

**Acknowledgment.** The authors appreciate helpful discussions with Professor C. D. Batich and Professor P. H. Holloway and data collection efforts of Dr. S.-P. Jeng and Dr. D. A. Asbury. This research was supported by the National Science Foundation through Grant No. CTS-9122575.

CM9701740